J. For. Res. (2023) 34:99–111
https://doi.org/10.1007/s11676-021-01438-1

ORIGINAL PAPER

Different hydraulic strategies under drought stress between *Fraxinus mandshurica* and *Larix gmelinii* seedlings

Dandan Luo[1,2] · Chuankuan Wang[1,2] · Ying Jin[1,2] · Zhimin Li[1,2] · Zhaoguo Wang[1,2]

Received: 3 April 2021 / Accepted: 14 November 2021 / Published online: 13 January 2022

Abstract Persistent and severe drought induced by global climate change causes tree mortality mainly due to the hydraulic imbalance of conduit systems, but the magnitude of injury may be species dependent. A water-exclusion experiment was carried out on seedlings of two tree species with distinct characteristics, i.e., *Fraxinus mandshurica* and *Larix gmelinii* to examine hydraulic responses of leaf, stem, and root to drought stress. The two species displayed different hydraulic strategies and related traits in response to drought stress. *L. gmelinii* reduced its leaf hydraulic conductance by quick stomatal closure and a slow decline in leaf water potential, with a more isohydric stomatal regulation to maintain its water status. In contrast, *F. mandshurica* was more anisohydric with a negative stomatal safety margin, exhibiting strong resistance to embolism in stem and leaf-stem segmentation of hydraulic vulnerability to preserve the hydraulic integrity of stem. These differences in hydraulic behaviors and traits between the two species in response to drought stress provide a potential mechanism for their co-existence in temperate forests, including which in the forest modeling would improve our prediction of tree growth and distribution under future climate change.

Keyword Embolism resistance · Hydraulic vulnerability · Stomatal safety margin · Stomatal regulation · Temperate species · Drought stress

Introduction

With ongoing global climate change, more frequent and extreme climate events and changes in precipitation patterns aggravate drought at both local and regional scales, leading to tree hydraulic dysfunction, carbon (C) imbalance, and eventual morality (McDowell et al. 2011; Allen et al. 2015; Clark et al. 2016). Catastrophic damage to hydraulic systems is a main cause of tree mortality during drought (Anderegg et al. 2016; Adams et al. 2017). However, tree responses to drought may vary with species that have different hydraulic characteristics and regulation strategies, even co-existing in the same ecosystem (Johnson et al. 2018). Therefore, it is critical to understand species-specific drought-response strategies and underlying mechanisms for accurately modeling and predicting tree growth and distribution under future climate change scenarios (Choat et al. 2018).

Trees adopt several trade-off strategies to cope with drought stress. Stomatal regulation is the first line of defense (Martínez-Vilalta and Garcia-Forner 2017). Plants can often be classified into isohydric and anisohydric species based on their stringency of stomatal limitation to transpiration in drying soils (Klein and Niu 2014; Martínez-Vilalta et al. 2014).

Project funding: This work was financially supported by the National Science and Technology Support Program of China (2011BAD37B01), the Program for Changjiang Scholars and Innovative Research Team in University (IRT_15R09), the National Key Research and Development Program of China (2016YFD0600201), and the Fundamental Research Funds for the Central Universities (2572018AA07).

The online version is available at http://www.springerlink.com.

Corresponding editor: Yanbo Hu.

✉ Chuankuan Wang
wangck@nefu.edu.cn

[1] Center for Ecological Research, Northeast Forestry University, 26 Hexing Road, Harbin 150040, People's Republic of China

[2] Key Laboratory of Sustainable Forest Ecosystem Management - Ministry of Education, Northeast Forestry University, Harbin 150040, People's Republic of China

Isohydric species have strict stomatal control to maintain a relatively constant minimum leaf water potential (Ψ_{leaf}) as soil water potential (Ψ_s) and/or vapor pressure deficit decline, while anisohydric species have a low stomatal sensitivity to environmental changes and allow Ψ_{leaf} to decline nearly parallel with Ψ_s as drought proceeds (Tardieu and Simonneau 1998; Klein and Niu 2014). However, plants often lie between these two extremes (Martínez-Vilalta et al. 2014). Previous syntheses suggest that the primary mechanisms of tree mortality, particularly under prolonged drought conditions, are different between isohydric and anisohydric species, that is, the former are mainly constricted by CO_2 assimilation due to earlier stomatal closure, whereas the latter have more resistant xylems to negative water potential and can maintain gas exchange under moderate drought stress (McDowell et al. 2008; Pou et al. 2012). However, Mitchell et al. (2013) reported that *Pinus radiata* D. Don (more isohydric) survived longer than two *Eucalyptus* species (more anisohydric) under drought because the former used the storage of nonstructural carbohydrates as a carbon source after stomatal closure, while the prolonged stomatal opening of the *Eucalyptus* led to more rapid water loss and thereafter, hydraulic failure.

Xylem embolism resistance is another mechanism of tree survival under drought stress. Embolism resistance has been characterized with several proxies for hydraulic failure, such as Ψ_{50} or Ψ_{88} (the water potential causing 50% or 88% loss of hydraulic conductivity; Brodribb and Cochard 2009; Choat et al. 2012), HSM (hydraulic safety margin, the difference between the minimum water potential (Ψ_{min}) and Ψ_{50} or Ψ_{88}; Anderegg et al. 2016; Adams et al. 2017), and SSM (stomatal safety margin, the difference between Ψg_{s88} (the leaf water potential causing 88% loss of the maximum stomatal conductance; Skelton et al. 2015) and Ψ_{50} or Ψ_{88}; Creek et al. 2018). Each proxy has its limitation that varies with species. For example, Ψ_{50} or Ψ_{88} often inaccurately represents tree drought tolerance because of interactions between stomatal regulation and xylem embolism (Blackman et al. 2009; Hochberg et al. 2017; Skelton et al. 2018); and conifers tend to have Ψ_{50} as the threshold, while angiosperms have Ψ_{88} (Choat et al. 20,122,018; Urli et al. 2013). Since Ψ_{min} integrates multiple responses of plant structure (e.g., rooting depth) and physiology (e.g., stomatal behavior) to environmental changes (Choat et al. 2012, 2018), it is difficult to quantify the influence of stomatal regulation on water potential, which leads to uncertainty of HSM-based prediction (Skelton et al. 2015; Chen et al. 2019). Moreover, the HSM for angiosperms is less than that for conifers, because the former has greater capacity to reverse embolism and riskier embolism threshold for survival (Choat et al. 2012, 2018; Urli et al. 2013). Chen et al. (2019) reported that SSM was a better predictor for the mortality of temperate broadleaf species than Ψ_{50}/Ψ_{88} and HSM because it integrates both stomatal regulation and xylem resistance and represents the degree of stomatal regulation over cavitation (Creek et al. 2018). Nevertheless, few verifications on SSM have been conducted.

Another strategy for plant mitigation of drought stress has been proposed as the within-plant hydraulic vulnerability segmentation, i.e., plants "sacrifice" their terminal organs (i.e., leaves and/or roots) in favor of the C-costly stems when stomatal regulation fails, maintaining a safe water balance (Tyree and Ewers 1991; Creek et al. 2018). However, there has been no generality on vulnerability segmentation reached to date (Pivovaroff et al., 2014). For example, Johnson et al. (2016) reported that the leaves and roots of four angiosperms and four conifers were more vulnerable than their trunks that were more vulnerable than their branches. However, Hao et al. (2013) found similar vulnerabilities across the organs of mature trees of *Betula papyrifera* Marsh. McCulloh et al. (2014) reported interspecific similarity but within-tree variability of vulnerability for large trees of four co-occurring conifers in western USA. Vulnerability segmentation is possibly species and/or age specific, and deserves more whole-plant studies.

Given the multiple mechanisms of hydraulic responses to drought, trees in natural settings display a suit of acclimatization and life-history strategies with different physiological, morphological, and anatomical traits (Choat et al. 2018), such as the "fast-slow" plant economics spectrum proposed by Reich (2014). Typically, angiosperms have higher water transport capacity and resource use efficiency to maintain faster growth rates, while gymnosperms have higher embolism resistance and less vulnerability to drought (Reich 2014; Jin et al. 2016).

In this study, a water-exclusion experiment was carried out with seedlings of Manchurian ash (*Fraxinus mandshurica* Rupr.) and Dahurian larch (*Larix gmelinii* (Rupr.) Rupr.) during the growing season of 2019 to examine dynamics in the hydraulics and related traits of roots, stems, and leaves. Ash and larch co-exist in Chinese temperate forests, and represent distinct plant functional types with contrasting anatomical, morphological, and physiological traits, e.g., a broadleaf angiosperm with ring-porous wood and wider and longer vessels versus an evergreen gymnosperm with nonporous wood and narrower and shorter tracheids. Our specific objectives were to: (1) examine temporal dynamics in hydraulics of the two species during the drought treatment; (2) explore leaf-stem-root hydraulic coordination in response to drought stress for the two species; and (3) compare their water regulation strategies under drought. We hypothesized that: (1) the hydraulic conductivity of both species would decline in response to drought stress but the magnitude of reduction would vary with species; (2) the two species would exhibit hydraulic vulnerability segmentation in response to severe drought, but with different temporal patterns; and (3) the two species would

develop distinct strategies of hydraulic regulation to cope with drought stress, with ash being more anisohydric and larch more isohydric.

Materials and methods

Study site and experimental design

Our study was carried out at the Maoershan Forest Ecosystem Research Station, Northeast China (45°20′ N, 127°30′ E, 400 m a.s.l.). This region is significantly influenced by a temperate continental monsoon climate, with humid, warm summers and dry, cold winters. Annual precipitation varies from 600 to 800 mm, of which ~ 62% falls during the growing season (June–September). Mean annual temperature is 3.1 °C, and January and July are the coldest and warmest months, with mean temperatures of − 18.5 °C and 22.0 °C, respectively. The frost-free period is 120–140 days (Wang et al. 2013).

Two-year-old seedlings of ash and larch were obtained from the local nursery and planted into individual pots (~22 L capacity), filled with soil from the adjacent forest in April 2019. The soil was passed through a 5-mm sieve and mixed well before using. At the beginning of the experiment, the seedlings were placed in an open area with full sunlight and watered 2–3 times per week to maintain soil moisture at ~ 80% of field capacity. In July 2019, four plants per species were randomly sampled to determine the background values of soil moisture and hydraulic variables of root, stem, and leaf. The plants were randomly assigned into two groups, i.e., treatment (SD) and control (CK). The SD group was left unwatered and blocked from rainfall using a transparent rain shelter to simulate drought, while the CK group was watered regularly as previous. As the experiment proceeded until almost completely dried out, the plants were sampled five times based on the continuously monitoring of soil volumetric water content (*VWC*) and physiological characteristics of the plants (Fig. 1). At each sampling period, eight plants per species were randomly sampled, of which four were used to measure predawn and midday leaf water potentials (Ψ_{PD} and Ψ_{MD}, respectively), and the rest four to in situ measure leaf stomatal conductance (g_s). The seedlings were brought back to the laboratory for measuring hydraulic conductivity of leaf, stem, and root. In general, the physiological responses of each plant were measured within the range of − 0.2 MPa to − 2.7 MPa of the plant water potential.

Measurements of leaf hydraulic traits

Pre-dawn and midday leaf water potential

Ψ_{PD} and Ψ_{MD} were measured on the same day, with the sampling times at predawn (03:00–05:00) and midday (12:00–14:00), respectively. The leaves of ash and leafy twigs of larch were excised from the plants and Ψ_{PD} and Ψ_{MD} were measured with a pressure chamber (Model 1505D; PMS Instrument Company, Albany, OR, USA). The relationship between Ψ_{PD} and Ψ_{MD} for each sampling time was fitted by Eq. (1) (Martínez-Vilalta et al. 2014):

$$\Psi_{MD} = \Lambda + \sigma\Psi_{PD} \quad (1)$$

where Λ is the intercept at $\Psi_{PD} = 0$, σ is the slope. Hydroscape area (HA) was fitted by the trajectory of Ψ_{MD} vs. Ψ_{PD} during soil drying (Meinzer et al. 2016; Fu et al. 2019).

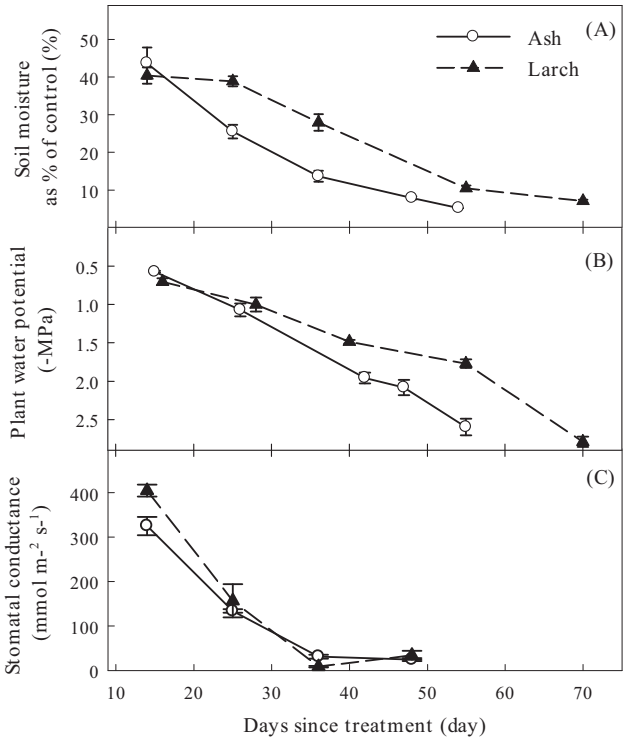

Fig. 1 Temporal dynamics in soil moisture (**A**), plant water potential (**B**), and stomatal conductance (**C**) for ash and larch along the drought-stress treatment. The error bars are standard errors ($n = 4$)

Pressure–volume (PV) curves

The PV curves of leaves were measured before the drought treatment. Four seedlings per species were randomly sampled and the leafy twigs of larch or the compound leaves with petioles of ash were excised from well-irrigated plants before dawn (03:00–05:00), immediately sealed in black plastic bags that contained moist filter paper and transported to the laboratory where they were rehydrated in deionised water for 30–60 min to full rehydration. They were then measured for saturated fresh weight with a digital balance (0.001 g resolution), and then immediately re-measured for

the initial leaf water potential (Ψ_{leaf}) with a pressure chamber. The leaves were dehydrated, and the mass and Ψ_{leaf} were repeatedly measured until the relationship between $1/\Psi_{leaf}$ and water loss at least five successive points became linear. The samples were then oven-dried at 70 °C for 48 h and weighed for dry mass. PV curves were established by plotting $1/\Psi_{leaf}$ against relative water content and used to calculate Ψ_{leaf} at turgor loss point (Ψ_{TLP}). Leaf capacitance (C_{leaf}) was calculated from the slope of the relationship between Ψ_{leaf} and water loss (Tyree and Hammel 1972).

Stomatal conductance (g_s)

Stomatal conductance was measured for the sun-exposed leaves between 08:00–10:00 a.m. using a LI-6400 portable photosynthesis (Li-6400; Li-Cor Inc., Lincoln, NE, USA), with the environmental settings as: the block temperature at 25 °C, the photosynthetically active radiation at 1200 mol m^{-2} s^{-1}, and the CO_2 concentration at 400 μmol mol^{-1}. The adjacent leaves or leafy twigs were then taken to measure Ψ_{leaf}. The relationship between g_s and Ψ_{leaf} (or Ψ_{PD}) for each sampling time was fitted by Eq. (2) (Blackman et al. 2019):

$$g_s = a/\left[1 + \exp(-(\Psi_{leaf} - x_0)/b)\right] \quad (2)$$

where a is the maximum g_s, b the coefficient determining the slope of the curve, and x_o the water potential causing 50% loss of stomatal conductance. A similar three-parameter sigmoidal function was used to fit the vulnerability curve of g_s, from which the leaf water potential and pre-dawn water potential causing 12% and 88% loss of stomatal conductance (Ψg_{s12} and Ψg_{s88}) were calculated, which represent the beginning of stomatal closure and complete closure, respectively (Skelton et al. 2015; Creek et al. 2018).

Measurements of whole-plant hydraulics and related traits

Hydraulic conductance (K)

The high-pressure flowmeter (HPFM) method (Hochberg et al. 2014) was used to measure the whole-plant hydraulics, because it is rapid and easy to operate in both laboratory and field. It can also be used to measure hydraulic conductance of the whole plant and organs (Tsuda and Tyree 1997), which considers both xylary and extra-xylary pathways for water. Hydraulic conductance was measured with an HPFM-Gen3 (Dynamax Corp., Houston, TX, USA). The sampled plants were moved to the laboratory before dawn (03:00–05:00) and covered with black plastic bags for 1.5 h to allow equilibration of the whole-plant water potential (Ψ_{plant}). The leaves or leafy twigs were cut to measure Ψ_{plant} and the wounds caused by water potential measurements were sealed with epoxy. Stems were then removed 5 cm above the soil surface, the cut end immediately submerged into deionized water and ~ 5 cm segments cut underwater. A bark strip (~3 cm in length) next to the cutting point was then removed to facilitate the connection to the HPFM tubing system. Shoot hydraulic conductance was measured using a quasi-steady-state measuring mode. The stem was connected with the HPFM and perfused at a pressure of ~0.5 MPa until a stable flow rate was reached (about 30–45 min). All the needles (for larch) or leaflets (for ash) were removed before stem hydraulic conductance was measured. The stable flow rate for stems was reached in 2–3 min. Root hydraulic conductance was measured using the transient measuring mode. The HPFM tubing system was connected to the remaining portion in the pot, and the applied pressure increased to 5 kPa s^{-1} while the pressure and flow rate were recorded every 2 s. Root hydraulic conductance was obtained from the slope of the linear part of the relationship between water flow rate and the applied pressure. Whole plant hydraulic resistance (R_{plant}, the inverse of plant hydraulics) was the sum of hydraulic resistance of shoot and root of each plant (i.e., $R_{plant} = R_{shoot} + R_{root}$), while leaf hydraulic resistance (R_{leaf}) was the difference between R_{shoot} and R_{stem} (Tsuda and Tyree 1997; Wang et al. 2016). Leaf area, stem length, and diameters at both ends of the stem were measured. The samples of leaf, stem, and root for each plant were then oven-dried at 70 °C for 72 h and weighed for dry mass. Leaf, stem, and root hydraulic conductance were expressed on a leaf area basis (K_{leaf}, K_{stem}, and K_{root}, respectively) for direct comparisons. The leaf specific hydraulic conductance of the CK group and the background values measured before the treatment were designated as the maximum plant hydraulic conductance (K_{max}). K_{leaf}, K_{stem}, and K_{root} during the whole drought treatment were correlated to the corresponding water potential.

The percentage loss in hydraulic conductivity (PLC) was calculated as:

$$PLC = 100 \times (1 - K/K_{max}) \quad (3)$$

The vulnerability curve for each species was fitted by the least square methods based on an empirical function (Tsuda and Tyree 1997) as:

$$PLC = a/(1 + exp(\, b(\Psi - c)) \quad (4)$$

where Ψ is plant water potential, a the maximum PLC, b the maximum slope of the curve, and c is Ψ_{50}. At the same time, the water potential associated with 12% and 88% loss of hydraulic conductivity (Ψ_{12} and Ψ_{88}) were calculated, which represent the thresholds of the beginning of K decline and plant death, respectively.

Wood density (WD) and root to shoot mass ratio (R/S)

Whole plants were harvested when the experiment was finished and separated into different biomass tissues. Each tissue from each plant was separately bagged, oven-dried at 70 °C for 48 h and weighed for dry mass. Stem volume was measured by the displacement method. WD was calculated as the dry mass of stem without bark divided by stem volume. R/S ratio was calculated as the ratio of the aboveground dry mass to the belowground.

Statistical analyses

Linear regression was used to fit the relationship between Ψ_{PD} and Ψ_{MD} within species, of which the intercept (Λ) and slope (σ) were used to determine the tendency in the isohydric to anisohydric continuum for each species (i.e., larger σ, more anisohydric; Martínez-Vilalta et al. 2014). The *t*-test was used to compare the initial traits of the two species. For each species, hydraulic conductivity was regressed against water potential with a three-parameter sigmoidal function, from which Ψ_{12}, Ψ_{50} and Ψ_{88} and their 95% confidence intervals (CIs) were obtained. Vulnerability segmentation for each species was assessed by the Ψ_{50} differences between leaf, root and stem ($\text{Leaf}\Psi_{50} - \text{Stem}\Psi_{50}$ and $\text{Root}\Psi_{50} - \text{Stem}\Psi_{50}$), i.e., vulnerability segmentation if the Ψ_{50} differences were greater than zero and their CIs did not overlap (Creek et al. 2018). The relationship between g_s and Ψ during drought was fitted with a three-parameter sigmoidal function, from which Ψg_{s12} and Ψg_{s88} (or ψg_{s12} and ψg_{s88}) were obtained. Stomatal safety margins (SSM_{50} or SSM_{88}) were calculated as the difference between Ψg_{s88} and Ψ_{50} or Ψ_{88} of leaf, stem, and root by species, respectively (Chen et al. 2019). Larger SSM_{50} or SSM_{88} values represented stronger stomatal regulation and xylem resistance coordination (Skelton et al. 2015). The loss of whole-plant hydraulic conductivity (%) and relative stomatal conductance (%) were fitted against the treatment duration (day) with a three-parameter sigmoidal function. The duration for plants to reach Ψg_{s88} and Ψ_{88} were defined as the times for stomatal closure and plant death threshold, respectively. All statistical analyses were performed in IBM SPSS Statistics 21.

Results

Temporal dynamics in hydraulics of ash and larch during drought-stress

As soil water content decreased along the drought-stress treatment (Fig. 1), g_s and hydraulic conductance of the two species declined but both exhibited distinct inter-specific temporal patterns (Fig. 2). The g_{s12} for ash occurred earlier than that for larch (Day 14 vs. Day 23), whereas g_{s88} for the former was later (Day 30 vs. Day 25). The duration between Ψg_{s12} and Ψg_{s88} was 16 days and two days for ash and larch, respectively. Conversely, Ψ_{50} and Ψ_{88} for ash occurred on Day 41 and Day 57, respectively, while those for larch occurred on Day 33 and Day 77, respectively. The duration between Ψ_{50} and Ψ_{88} was 16 and 43 days for ash and larch, respectively.

Water potential of leaf, stem, and root and whole-plant water transport efficiency for both species also decreased as drought-stress increased, but the thresholds of stomatal closure and vulnerability varied with species and organs (Figs. 3 and 4). Specifically, the Ψg_{s88} for ash (-1.52 ± 0.06 MPa) was more negative than for larch (-1.40 ± 0.04 MPa), while the Ψg_{s12} for the former (-0.92 ± 0.06 MPa) was less negative than that of the later (-1.22 ± 0.04 MPa) (Fig. 3A and C). The ψg_{s88} for ash (-1.59 ± 0.06 MPa) was more negative than that for larch (-0.89 ± 0.04 MPa) (Fig. 3B and D). The whole-plant Ψ_{50} for larch (-1.64 ± 0.07 MPa) was higher than that for ash (-1.85 ± 0.11 MPa) (Fig. 4A and B). The stem Ψ_{50} and Ψ_{88} for ash (-2.13 ± 0.11 and -2.63 ± 0.11 MPa) were more negative than those for larch (-1.70 ± 0.07 and -1.85 ± 0.07 MPa) (Fig. 4E and F). The root Ψ_{88} for ash was lower than that for larch, but an opposite trend occurred for leaf Ψ_{50} (Fig. 4C and D). The difference between Ψ_{50} and Ψ_{88} was the least for stems, followed by leaves, and the greatest for roots; the whole-plant difference for ash was greater than that for larch. Ash, rather than larch, showed a vulnerability segmentation with leaf Ψ_{50} > root Ψ_{50} > stem Ψ_{50} and non-overlapped CIs of Ψ_{50} for ash, but overlapped CIs of Ψ_{50} for larch despite $\text{leaf}\Psi_{50} > \text{root}\Psi_{50} > \text{stem}\Psi_{50}$ (Fig. 4).

Comparisons of hydraulics and related traits between ash and larch

Hydraulics and related traits differed significantly between the two species (Figs. 5 and 6). Specifically, the means of Ψ_{PD}, Ψ_{MD}, and Ψ_{TLP} were significantly ($P < 0.05$) higher (less negative) for ash than for larch, while that of g_s was significantly lower for the former than for the latter. The K_{leaf}, K_{stem}, and K_{root} for ash were 6.7, 2.6, and 2.7 times greater than those for larch, respectively. The C_{leaf} for larch was 2.3 times greater than that for ash, but the *WD* and R/S ratio for ash (0.59 g cm^{-3} and 1.1) were significantly greater ($P < 0.05$) than those for larch (0.41 g cm^{-3} and 0.5).

The relationship of Ψ_{MD} to Ψ_{PD} was different between ash and larch (Fig. 7). The slope of the relationship for ash (0.91) was insignificant from 1 (0.91 [0.77, 1.06]), while that for larch was significantly less than 1 (0.69 [0.59, 0.81]). The intercept for ash (-0.64) was larger (less negative) than that for larch (-0.94). HA was 1.17

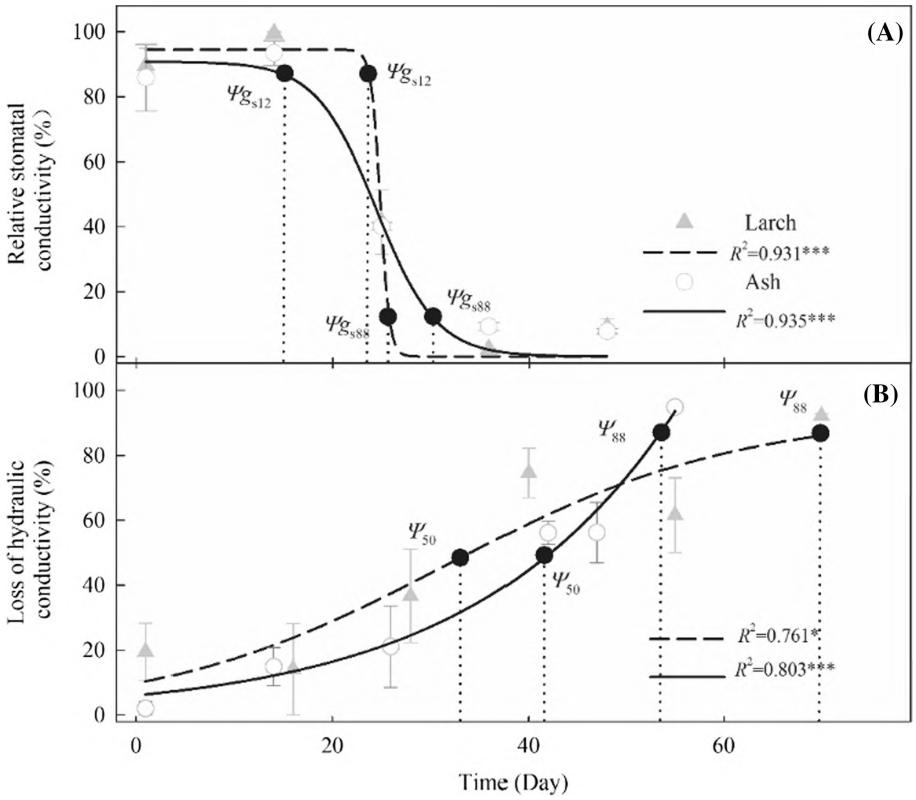

Fig. 2 Temporal dynamics in relative stomatal conductance (**A**) and loss of plant hydraulic conductivity (**B**) for ash and larch along the drought-stress treatment. The dotted lines represent the time when the water potential caused 12% and 88% loss of stomatal conductance (Ψg_{s12} and Ψg_{s88}), and 50% and 88% loss of plant hydraulic conductance (Ψ_{50} and Ψ_{88}) occurred, respectively. *$P<0.05$, ***$P<0.0001$

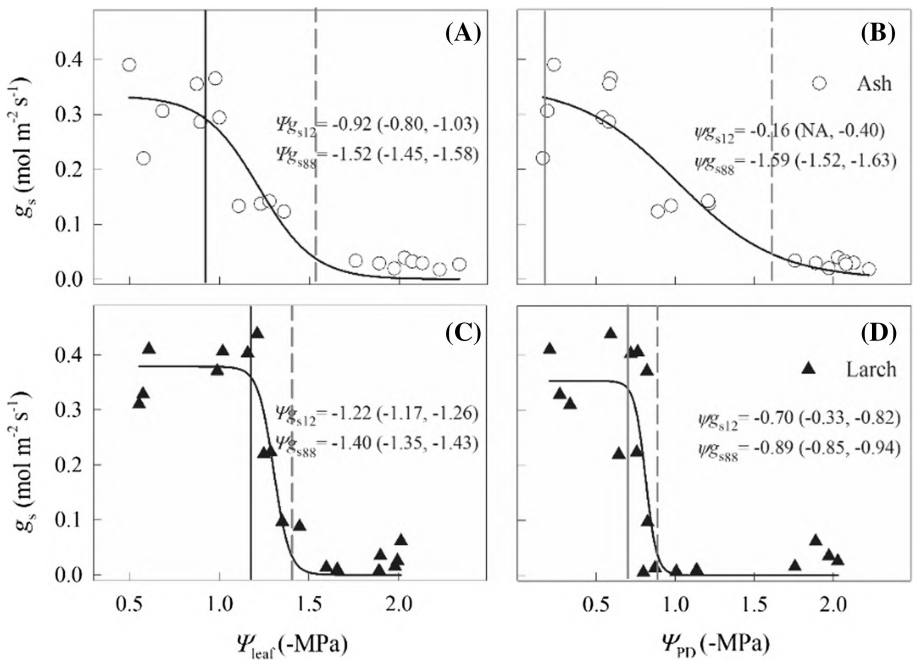

Fig. 3 Responses of stomatal conductance to decreasing leaf water potential (Ψ_{leaf}) and pre-dawn water potential (Ψ_{PD}) for ash (**A**, **B**) and larch (**C**, **D**). The vertical solid and dashed lines indicate the leaf water potential (Ψg_{s12} and Ψg_{s88}) and pre-dawn water potential (ψg_{s12} and ψg_{s88}) at 12% and 88% loss of stomatal conductance, respectively. The values in parentheses are 95% confidence intervals

for larch and 1.68 for ash. Moreover, leaf SSM_{50} was less than 0 for ash but greater than 0 for larch. However, leaf SSM_{88} was comparable between the two species (0.45 vs. 0.48) (Fig. 8). Both SSM_{50} and SSM_{88} of the stem and whole plant for ash were greater than those for larch. Nevertheless, ash had less root SSM_{50} than larch (0.19 vs. 0.22) but greater root SSM_{88} (1.35 vs. 0.60). The SSM_{88} of leaf, stem, root, and whole plant for ash were much higher than those for larch.

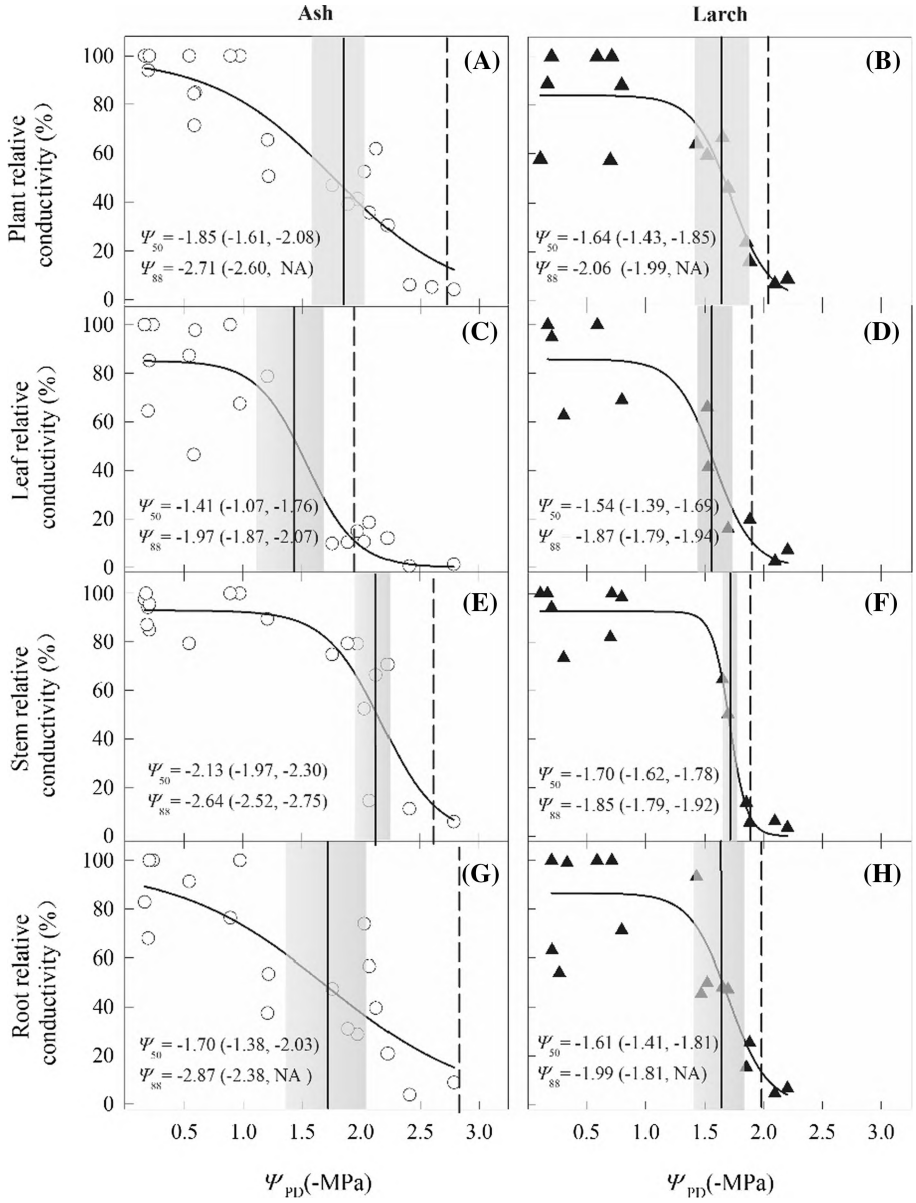

Fig. 4 Hydraulic vulnerability curves showing responses of the relative conductivity of whole plant (**A**, **B**), leaf (**C**, **D**), stem (**E**, **F**), and root (**G**, **H**) to respective pre-dawn water potential (Ψ_{PD}) for ash and larch. The vertical solid lines indicate the water potential causing 50% loss of conductance (Ψ_{50}) and the shaded areas represent 95% confidence interval. The vertical dashed lines represent the water potential causing 88% loss of conductance (Ψ_{88})

Discussion

Temporal dynamics in hydraulics of ash and larch during drought stress

As drought stress increased, stomatal closure occurred early but slowly for ash while it occurred late but rapidly for larch. Consequently, the duration of stomatal closure for ash lasted eight times longer than that for larch (Fig. 2). These patterns suggest that larch has a more isohydric regulation, while ash is more anisohydric. Both leaf and stem Ψ_{50} for larch occurred after Ψ_{gs88} (Figs. 3 and 4), suggesting that leaf hydraulic function is maintained to some extent even after stomatal closure, which consequently slows down the decline in plant dehydration and water potential. For ash, however, the Ψ_{50} of the stem rather than the Ψ_{50} of leaf occurred after Ψ_{gs88} (Figs. 3 and 4), suggesting that the decline in K_{leaf} causes partial/complete stomatal closure and thereby maintains the hydraulic function of the stem. After stomatal closure, water potential continued to decrease slowly and hydraulic conductivity loss increased (Fig. 2), possibly resulting from water loss via cuticular conductance, stomatal leaking and through other tissues such as bark (Choat et al. 2018).

The distinct temporal patterns of hydraulics under drought-stress between ash and larch may be attributed to several factors. First, larch has a smaller K_{leaf} and total leaf area with less water loss through the epidermis compared with ash (Fig. 5; Reich 2014). Second, the higher stem Ψ_{50} and less stem safety margin of larch (Figs. 4 and 8B) suggest

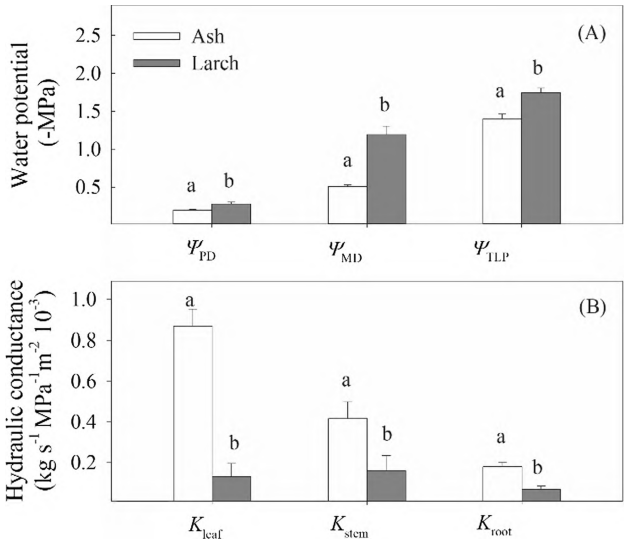

Fig. 5 Comparisons of hydraulics traits between ash and larch without drought stress. Ψ_{PD}, Ψ_{MD}, and Ψ_{TLP} represent predawn, midday, and turgor loss point water potential, respectively; K_{leaf}, K_{stem}, and K_{root} represent leaf-area-based hydraulic conductance of stem, leaf, and root, respectively. Different letters above the bars (mean ± SE, $n=4$) indicate significant differences between the two species ($\alpha=0.05$)

its greater stem water storage and hydraulic capacitance (Meinzer et al. 2009). The release of stored water can supply the transpiration stream and buffer the decline of water potential (Choat et al. 2018) induced by drought stress, and consequently reduce the decreases in K_{plant} and water potential (Borchert and Pockman 2005). Third, ash consumed water faster than larch as drought stress increased (Figs. 1 and 2), evidenced by its greater Ψ_{PD} and R/S ratio (Figs. 5 and 6) and the longer period of its stomatal opening (Figs. 2 and 3). The greater Ψ_{PD} of ash possibly resulted from its larger rooting-zone that translated more soil water into Ψ_{PD}, while the longer period of stomatal opening likely depleted more soil water, resulting in faster reduction in Ψ_{PD} over time (Sperry et al. 2002; Martínez-Vilalta and Garcia-Forner 2017; Nolan et al. 2017b). Nevertheless, it should be noted that our potted experiment may limit the development of seedling rooting systems (Yoseph et al. 2011; Nardini et al. 2016), which therefore requires more field studies.

Leaf-stem-root hydraulic coordination of ash and larch in response to drought stress

Hydraulic vulnerability segmentation often promotes plant physiological recovery once soil rehydrates (Ishida et al. 2008) and reflects the combination of plant hydraulics and C economies (Sperry 2000). In this study, a leaf-stem vulnerability segmentation occurred for ash but not for larch (Fig. 3), which contradicts a previous study in the same area (Jin et al. 2019). The contradiction may be associated with tree status and experimental protocols. Unlike our drought-stress treatment of seedlings, Jin et al (2019) investigated mature trees under natural settings where water availability may not have been a limiting factor. They also

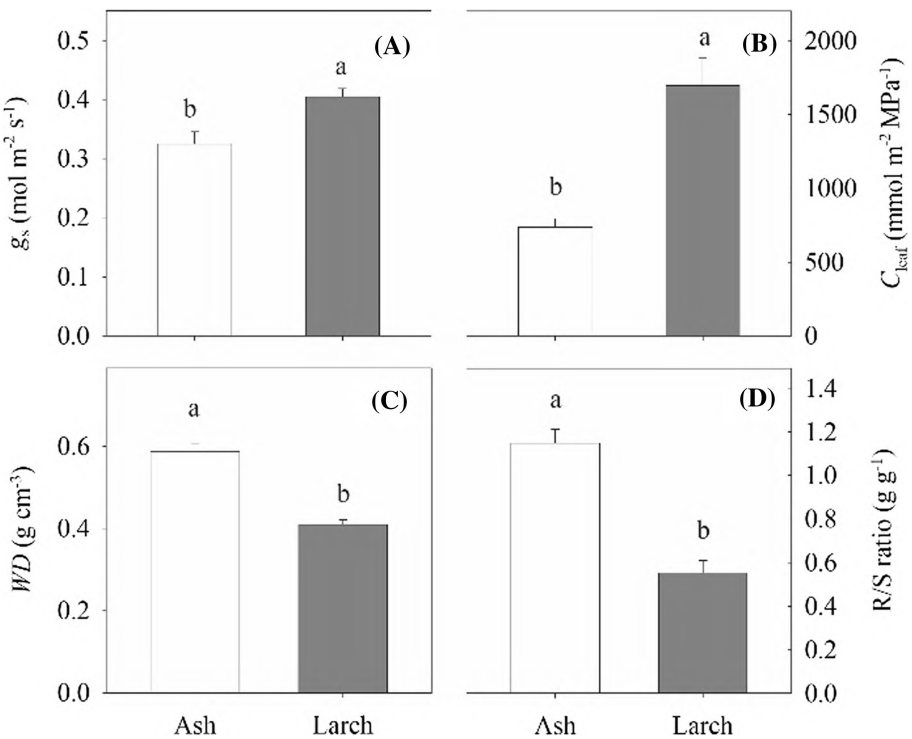

Fig. 6 Comparisons of hydraulic-related traits between ash and larch without drought stress; g_s, stomatal conductance; C_{leaf}, leaf capacitance; *WD*, wood density; R/S ratio, root to shoot mass ratio. Different letters above the bars (mean ± SE, $n=4$) indicate significant differences between the two species ($\alpha=0.05$)

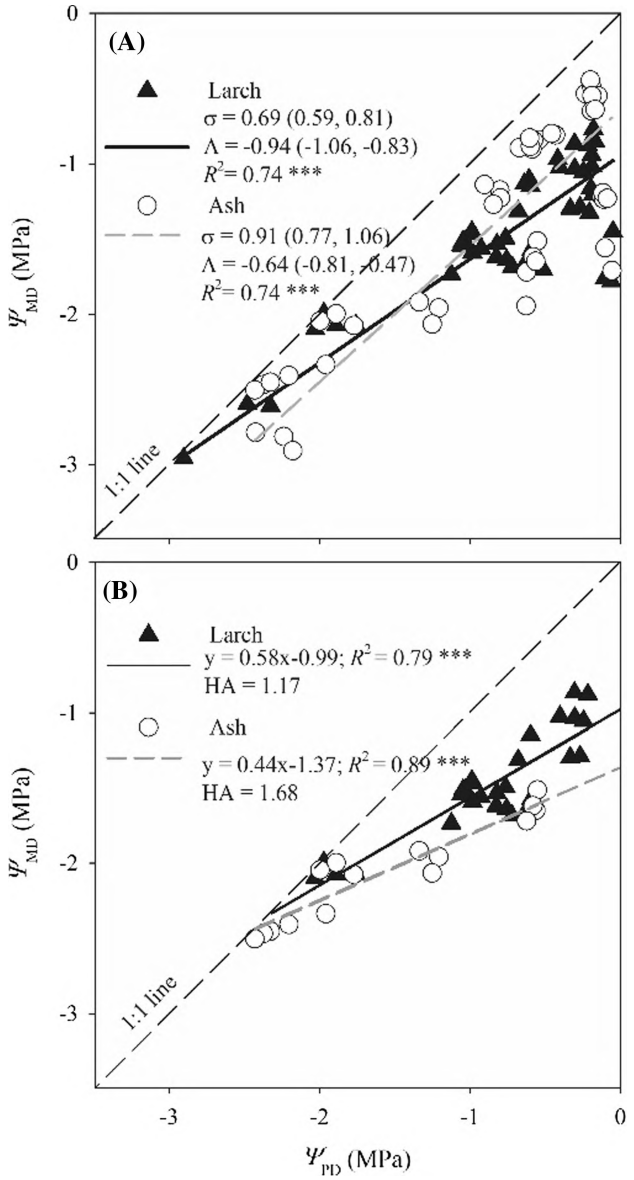

Fig. 7 Relationships between predawn (Ψ_{PD}) and midday leaf water potential (Ψ_{MD}). (**A**) Including all the data; (**B**) stomatal regulation of Ψ_{MD} prior to complete stomatal closure. HA is hydroscape area. The regression equations (including R^2) are given. *** $P < 0.0001$

used the timed-rehydration method to measure K_{leaf} and construct vulnerability curves, while we were measured along a drought-stress process. They measured the hydraulic conductivity and vulnerability of stems without bark, while we measured the vulnerability of stems with bark that included both xylary and extra-xylary pathways. Nevertheless, it should be noted that the high-pressures applied in our HPFM measurements might remove some of the xylary embolism, although the HPFM and conventional evaporative flux methods were demonstrated to yield consistent values of plant hydraulic resistances (Tsuda and Tyree 1997). In addition, the leaves of larch from different nodal positions, basal versus apical leaves, had varied vulnerability, in line with previous studies (e.g., Hochberg et al. 2017). When the water potential drops low enough, trees can massively shed basal leaves while retaining apical leaves, and leaf embolism resistance to drought can be enhanced by osmotic regulation. This may result in the smaller embolization differences between the stem and leaves for larch (Fig. 4).

Although the stem Ψ_{50} of ash was more negative than that of larch, its leaf Ψ_{50} was slightly higher, which may be caused by higher leaf Ψ_{TLP}. When Ψ_{leaf} drops close to Ψ_{TLP}, the extra-xylary conductance decreases, leading to leaf hydraulic dysfunction (Blackman et al. 2010). The decoupling of stem and leaf embolism resistance suggests that these traits may have evolved independently, and the multiple combinations may reflect the diversity of drought strategies (Pivovaroff et al. 2016; Laughlin et al. 2020).

Nevertheless, no root-stem vulnerability segmentation under drought stress was detected for ash or larch (Fig. 4), illustrating that water movement between root and stem is coupled more strongly than that between leaf and stem. Collectively, hydraulic vulnerability varies with species, organ, and the environmental conditions, highlighting the importance of considering multiple factors in assessing tree resistance to and recovery from drought.

Water regulation strategies of ash and larch under drought stress

Occupying different ecohydrological niches is a primary mechanism of resource partitioning for co-existing species, among which differing responses of stomatal conductance to variations in soil water content (i.e., isohydric/anisohydric continuum) is an important strategy (Nolan et al. 2017a). Within the tolerance of hydraulic systems, stomatal regulation takes full advantage of the range of xylem pressure (Choat et al. 2012). In this study, larch is classified as more isohydric while ash is more anisohydric based on three metrics. First, the σ for ash was close to 1, while that for larch was less than 1 (Fig. 7; strict isohydric ($\sigma = 0$), partial isohydric ($0 < \sigma < 1$), strict anisohydric ($\sigma = 1$), extreme anisohydric ($\sigma > 1$); Martínez-Vilalta et al. 2014). This result for *Fraxinus mandchurica* agrees with previous studies for *F. excelsior* and *F. americana* (Gu et al. 2015; Leuschner et al. 2019), but for *Larix gmelinii,* it is inconsistent with other larch species. For example, *L. kaempferi* sustained Ψ_{leaf} and showed an isohydric stomatal regulation (Bhusal et al. 2020; Sasani et al. 2021), while *L. decidua* was considered anisohydric (Streit et al. 2014; Sasani et al. 2021) or isohydric (Peters et al. 2019). The second metric used was the hydroscape area (HA) that integrates multiple mechanisms of regulating Ψ_{plant} and stomatal behavior during soil drying (Meinzer et al. 2016; Fu and Meinzer 2019; Li et al. 2019).

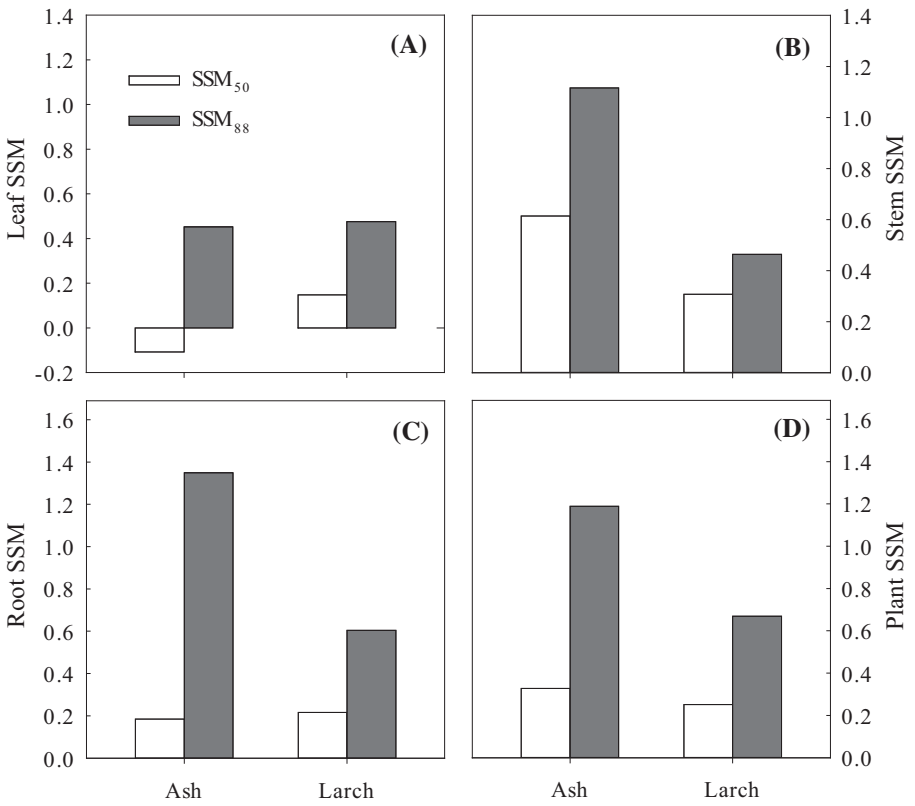

Fig. 8 Comparisons of stomatal safety margins (SSM) at leaf (**A**), stem (**B**), root (**C**), and whole-plant (**D**) levels between ash and larch. SSM_{50} or SSM_{88} is the difference in the water potential between causing 88% loss of stomatal conductance (Ψg_{s88}) and 50% or 88% loss of hydraulic conductance (Ψ_{50} and Ψ_{88})

Ash had a larger HA than larch (1.68 cf. 1.17), showing an anisohydric tendency. Based on SSM_{50} (Skelton et al. 2015), ash was also defined as anisohydric (negative leaf SSM_{50}) while larch was isohydric (positive leaf SSM_{50}; Fig. 8).

In addition to stomatal regulation, embolism resistance to drought is another key strategy for co-existing species to avoid direct competitive interactions. The stomatal safety margin (SSM) has been suggested as a good proxy for characterizing tree hydraulic dysfunction (Chen et al. 2019) because it is jointly controlled by stomatal sensitivity and xylem embolism resistance to drought. In this study, larch had a higher leaf SSM_{50} and longer survival period under drought stress than ash, consistent with the findings of Chen et al. (2019), but larch had lower stem and whole-plant SSM (Fig. 8). Theoretically, angiosperms show hydraulic failure with more negative stem water potential (i.e., Ψ_{88}) than conifers (i.e., Ψ_{50}; Urli et al. 2013). In our case, the Ψ_{88} and SSM_{88} of stem and whole plant for ash were much higher than the Ψ_{50} and SSM_{50} for larch. This suggests that ash has much higher embolism resistance and a wider safety margin than larch. These results also show that ash had a significant hydraulic vulnerability segmentation, which may be another strategy to prevent excessive embolization.

Additionally, the difference in SSM between ash and larch may be attributed to their ability of embolism repair and other traits (e.g., wood density, hydraulic capacitance). The Ψ_{88} of leaf, stem, and roots were comparable for larch but significantly different for ash, suggesting that ash may have greater regeneration capacity after experiencing a severe drought. This repair ability may be associated with the content of nonstructural carbohydrates that can induce an osmotic gradient to drive refilling of embolized vessels (Adams et al. 2017). Ash may have weaker repair ability due to lower sugar concentrations in the stem than larch (unpublished data). Additionally, larch had less WD and embolism resistance of root, stem, and whole plant to drought (i.e., less negativeΨ_{50} and Ψ_{88}) than ash (Figs. 4 and 6), in agreement with previous studies (Klein and Niu 2014; Martínez-Vilalta et al. 2014; Fu and Meinzer 2019). The larger WD and stem SSM of ash resulted in a smaller stem hydraulic capacitance (Fu et al. 2019). Along the iso-anisohydric continuum, there is a tendency for decreasing reliance on capacity to buffer changes in xylem tension to avoid embolism and increasing reliance on structural reinforcement of xylem to resist embolism (Yi et al. 2017; Fu and Meinzer 2019). It is also suggested that high leaf capacitance is correlated with slow stomatal closure (Martins et al. 2016), and leaf and stem capacitance may be inversely related (Fu et al. 2019). But in this study, the C_{leaf} of larch was higher than that of ash, which confers a protection mechanism to avoid Ψ_{leaf} decline. The lower C_{leaf} allows ash to have a higher capacity of foliar water uptake (Berry et al. 2019) and to mitigate the decline in K_{plant} and Ψ_{leaf} (Fuenzalida et al. 2019; Binks

et al. 2020), which makes the Ψ_{50} of ash reached later than larch (Fig. 2B).

Larch and ash diverge their hydraulic strategies under drought stress. Larch displays a conservative strategy but a risky C economy with isohydric regulation, low embolism resistance and no leaf-stem vulnerability segmentation. Conversely, ash shows a risky hydraulic strategy with anisohydric behavior, high embolism resistance, and leaf-stem vulnerability segmentation. Such hydraulic differentiations facilitate species coexistence (Nolan et al. 2017a) and productivity maintenance (Roman et al. 2015) under drought conditions.

Conclusions

Our water-exclusion experiment on Manchurian ash and Dahurian larch seedlings displayed contrasting responses of hydraulic and water regulation strategies to drought stress, which provide potential mechanisms for their co-existence. Larch mainly uses stomata as a "safety valve" to maintain hydraulic functions of the whole plant and delays dehydration time under drought; ash uses leaves as "hydraulic fuses" (i.e., leaf-stem vulnerability segmentation) to preserve the hydraulic integrity of the stem. Larch adopts drought avoidance and an isohydric strategy with strong stomatal sensitivity, while ash is more anisohydric with a strong drought resistance. Hydraulic coordination among different organs is central to our understanding of how trees and forest communities respond to drought, and the occupation of ecohydrological niches by co-existing species is a primary strategy for their resource partitioning in the ecosystem (Peñuelas et al. 2011; Yoseph et al. 2011). Our findings highlight the significance of considering different hydraulic responses of co-existing species in modelling and prediction of tree growth, survival, and distribution under global climate changes.

References

Adams HD, Zeppel MJB, Anderegg WRL, Hartmann H, Landhäusser SM, Tissue DT, Huxman TE, Hudson PJ, Franz TE, Allen CD, Anderegg LDL, Barron-Gafford GA, Beerling DJ, Breshears DD, Brodribb TJ, Bugmann H, Cobb RC, Collins AD, Dickman LT, Duan H, Ewers BE, Galiano L, Galvez DA, Garcia-Forne N, Gaylord ML, Germino MJ, Gessler A, Hacke UG, Hakamada R, Hector A, Jenkins MW, Kane JM, Kolb TE, Law DJ, Lewis JD, Limousin JM, Love DM, Macalady AK, Martínez-Vilalta J, Mencuccini J, Mitchell PJ, Muss JD, O'Brien MJ, O'Grady AP, Pangle RE, Pangle EA, Piper FI, Plaut JA, Pockman WT, Quirk J, Reinhardt K, Ripullone F, Ryan MG, Sala A, Sevanto S, Sperry JS, Vargas R, Vennetier M, Way DA, Xu CG, Yepez EA, McDowell NG (2017) A multispecies synthesis of physiological mechanisms in drought-induced tree mortality. Nat Ecol Evol 1:1285–1291

Allen CD, Breshears DD, Mcdowell NG (2015) An underestimation of global vulnerability to tree mortality and forest die-off from hotter droughts in the Anthropocene. Ecosphere 6:1–55

Anderegg WR, Klein T, Bartlett M, Sack L, Pellegrini AF, Choat B, Jansen S (2016) Meta-analysis reveals that hydraulic traits explain cross-species patterns of drought-induced tree mortality across the globe. Proc Natl Acad Sci USA 113:5024–5029

Berry ZC, Emery NC, Gotsch SG, Goldsmith GR (2019) Foliar water uptake: processes, pathways, and integration into plant water budgets. Plant Cell Environ 42:410–423

Bhusal N, Lee M, Han AR, Han A, Kim HS (2020) Responses to drought stress in *Prunus sargentii* and *Larix kaempferi* seedlings using morphological and physiological parameters. For Ecol Manag 465:118099

Binks O, Coughlin I, Mencuccini M, Meir P (2020) Equivalence of foliar water uptake and stomatal conductance? Plant Cell Environ 43:524–528

Blackman CJ, Brodribb TJ, Jordan GJ (2009) Leaf hydraulics and drought stress: response, recovery and survivorship in four woody temperate plant species. Plant Cell Environ 32:1584–1595

Blackman CJ, Brodribb TJ, Jordan GJ (2010) Leaf hydraulic vulnerability is related to conduit dimensions and drought resistance across a diverse range of woody angiosperms. New Phytol 188:1113–1123

Blackman CJ, Creek D, Maier C, Aspinwall MJ, Drake JE, Pfautsch S, O'Grady A, Delzon S, Medlyn BE, Tissue DT, Choat B (2019) Drought response strategies and hydraulic traits contribute to mechanistic understanding of plant dry-down to hydraulic failure. Tree Physiol 39:910–924

Borchert R, Pockman WT (2005) Water storage capacitance and xylem tension in isolated branches of temperate and tropical trees. Tree Physiol 25:457–466

Brodribb TJ, Cochard H (2009) Hydraulic failure defines the recovery and point of death in water-stressed conifers. Plant Physiol 149:575–584

Chen ZC, Li S, Luan JW, Zhang YT, Zhu SD, Wan XC, Liu SR (2019) Prediction of temperate broadleaf tree species mortality in arid limestone habitats with stomatal safety margins. Tree Physiol 39:1428–1437

Choat B, Brodribb TJ, Brodersen CR, Duursma RA, López R, Medlyn BE (2018) Triggers of tree mortality under drought. Nature 558:531–539

Choat B, Jansen S, Brodribb TJ, Cochard H, Delzon S, Bhaskar R, Bucci SJ, Field TS, Gleason SM, Hacke UG, Jacobsen AL, Jacobsen F, Maherali H, Martinez-Vilalta J, Mayr S, Mencuccini M, Mitchell PJ, Nardini A, Pittermann J, Pratt RB, Sperry JS, Westoby M, Wright IJ, Zanne AE (2012) Global convergence in the vulnerability of forests to drought. Nature 491:752–755

Clark JS, Iverson LR, Woodall CW, Allen GD, Bell DM, Bragg DC, D'Amato A, Davis FW, Hersh M, Ibanez I, Jackson ST, Matthews S, Pederson N, Peters MP, Schwartz MW, Waring KM, Zimmermann NE (2016) The impacts of increasing drought on forest dynamics, structure, and biodiversity in the United States. Glob Chang Biol 22:2329–2352

Creek D, Blackman C, Brodribb TJ, Choat B, Tissue DT (2018) Coordination between leaf, stem and root hydraulics and gas exchange in three arid-zone angiosperms during severe drought and recovery. Plant Cell Environ 41:2869–2881

Fu XL, Meinzer FC (2019) Metrics and proxies for stringency of regulation of plant water status (iso/anisohydry): a global data set reveals coordination and tradeoffs among water transport traits. Tree Physiol 39:122–134

Fu XL, Meinzer FC, Woodruff DR, Liu YY, Smith DD, McCulloh KA, Howard AR (2019) Coordination and trade-offs between leaf and stem hydraulic traits and stomatal regulation along a spectrum of isohydry to anisohydry. Plant Cell Environ 42:2245–2258

Fuenzalida TI, Bryant CJ, Ovington LI, Yoon HJ, Oliveira RS, Sack L, Ball MC (2019) Shoot surface water uptake enables leaf hydraulic recovery in *Avicennia marina*. New Phytol 224:1504–1511

Gu L, Pallardy SG, Hosman KP, Sun Y (2015) Predictors and mechanisms of the drought-influenced mortality of tree species along the isohydric to anisohydric continuum in a decade-long study of a central US temperate forest. Biogeosci Discuss 12:1285–1325

Hao GY, Wheeler JK, Holbrook NM, Goldstein G (2013) Investigating xylem embolism formation, refilling and water storage in tree trunks using frequency domain reflectometry. J Exp Bot 64:2321–2332

Hochberg U, Degu A, Gendler T, Fait A, Rachmilevitch S (2014) The variability in the xylem architecture of grapevine petiole and its contribution to hydraulic differences. Funct Plant Biol 42:357–365

Hochberg U, Windt CW, Ponomarenko A, Zhang YJ, Gersony J, Rockwell FE, Holbrook NM (2017) Stomatal closure, basal leaf embolism, and shedding protect the hydraulic integrity of grape stems. Plant Physiol 174:764–775

Ishida A, Nakano T, Yazaki K, Matsuki S, Koike N, Lauenstein DL, Shimizu M, Yamashita N (2008) Coordination between leaf and stem traits related to leaf carbon gain and hydraulics across 32 drought-tolerant angiosperms. Oecologia 156:193–202

Jin Y, Wang CK, Zhou ZH (2019) Conifers but not angiosperms exhibit vulnerability segmentation between leaves and branches in a temperate forest. Tree Physiol 39:454–462

Jin Y, Wang CK, Zhou ZH, Li ZM (2016) Coordinated performance of leaf hydraulics and economics in 10 Chinese temperate tree species. Funct Plant Biol 43:1082–1090

Johnson DM, Domec J, Berry ZC, Schwantes AM, McCulloh KA, Woodruff DR, Polley HW, Wortemann R, Swenson JJ, Mackay DS, McDowell NG, Jackson RB (2018) Cooccurring woody species have diverse hydraulic strategies and mortality rates during an extreme drought. Plant Cell Environ 41:576–588

Johnson DM, Wortemann R, McCulloh KA, Jordan-Meille L, Ward E, Warren JM, Palmroth S, Domec JC (2016) A test of the hydraulic vulnerability segmentation hypothesis in angiosperm and conifer tree species. Tree Physiol 36:989–993

Klein T, Niu S (2014) The variability of stomatal sensitivity to leaf water potential across tree species indicates a continuum between isohydric and anisohydric behaviors. Funct Ecol 28:1313–1320

Laughlin DC, Delzon S, Clearwater M, Bellingham PJ, McGlone MS, Richardson SJ (2020) Climatic limits of temperate rainforest tree species are explained by xylem embolism resistance among angiosperms but not among conifers. New Phytol 226:727–740

Leuschner C, Wedde P, Lübbe T (2019) The relation between pressure–volume curve traits and stomatal regulation of water potential in five temperate broadleaf tree species. Ann for Sci 76:60

Li XM, Blackman CJ, Peters JMR, Choat B, Rymer PD, Medlyn BE, Tissue DT (2019) More than iso/anisohydry: Hydroscapes integrate plant water use and drought tolerance traits in 10 eucalypt species from contrasting climates. Funct Ecol 33:1035–1049

Martínez-Vilalta J, Garcia-Forner N (2017) Water potential regulation, stomatal behaviour and hydraulic transport under drought: deconstructing the iso/anisohydric concept. Plant Cell Environ 40:962–976

Martínez-Vilalta J, Poyatos R, Aguade D, Retana J, Mencuccini M (2014) A new look at water transport regulation in plants. New Phytol 204:105–115

Martins SCV, McAdam SAM, Deans RM, DaMatta FM, Brodribb TJ (2016) Stomatal dynamics are limited by leaf hydraulics in ferns and conifers: results from simultaneous measurements of liquid and vapour fluxes in leaves. Plant Cell Environ 39:694–705

McCulloh KA, Johnson DM, Meinzer FC, Woodruff DR (2014) The dynamic pipeline: hydraulic capacitance and xylem hydraulic safety in four tall conifer species. Plant Cell Environ 37:1171–1183

McDowell N, Pockman WT, Allen CD, Breshears DD, Cobb N, Kolb T, Plaut J, Sperry J, West A, Williams DG, Yepez EA (2008) Mechanisms of plant survival and mortality during drought: why do some plants survive while others succumb to drought? New Phytol 178:719–739

McDowell NG, Beerling DJ, Breshears DD, Fisher RA, Raffa KF, Stitt M (2011) The interdependence of mechanisms underlying climate-driven vegetation mortality. Trend Ecol Evol 26:523–532

Meinzer FC, Johnson DM, Lachenbruch B, McCulloh KA, Woodruff DR (2009) Xylem hydraulic safety margins in woody plants: coordination of stomatal control of xylem tension with hydraulic capacitance. Funct Ecol 23:922–930

Meinzer FC, Woodruff DR, Marias DE, Smith DD, Mcculloh KA, Howard AR, Magedman AL (2016) Mapping 'hydroscapes' along the iso- to anisohydric continuum of stomatal regulation of plant water status. Ecol Lett 19:1343–1352

Mitchell PJ, O'Grady AP, Tissue DT, White DA, Ottenschlaeger ML, Pinkard EA (2013) Drought response strategies define the relative contributions of hydraulic dysfunction and carbohydrate depletion during tree mortality. New Phytol 197:862–872

Nardini A, Casolo V, Dal Borgo A, Savi T, Stenni B, Bertoncin P, Zini L, McDowell NG (2016) Rooting depth, water relations and non-structural carbohydrate dynamics in three woody angiosperms differentially affected by an extreme summer drought. Plant Cell Environ 39:618–627

Nolan RH, Fairweather KA, Tarin T, Santini NS, Cleverly J, Faux R, Eamus D (2017a) Divergence in plant water-use strategies in semiarid woody species. Funct Plant Biol 44:1134–1146

Nolan RH, Tarin T, Santini NS, Mcadam S, Ruman R, Eamus D (2017b) Differences in osmotic adjustment, foliar ABA dynamics and stomatal regulation between an isohydric and anisohydric woody angiosperm during drought. Plant Cell Environ 40:3122–3134

Ocheltree TW, Nippert JB, Prasad PV (2016) A safety vs. efficiency trade-off identified in the hydraulic pathway of grass leaves is decoupled from photosynthesis, stomatal conductance and precipitation. New Phytol 210:97–107

Peñuelas J, Terradas J, Lloret F (2011) Solving the conundrum of plant species coexistence: water in space and time matters most. New Phytol 189:5–8

Peters RL, Speich M, Pappas C, Kahmen A, von Arx G, Pannatier EG, Steppe K, Treydte K, Stritih A, Fonti P (2019) Contrasting stomatal sensitivity to temperature and soil drought in mature alpine conifers. Plant Cell Environ 42:1674–1689

Pivovaroff AL, Pasquini SC, De Guzman ME, Alstad KP, Stemke JS, Santiago LS (2016) Multiple strategies for drought survival among woody plant species. Funct Ecol 30:517–526

Pivovaroff AL, Sack L, Santiago LS (2014) Coordination of stem and leaf hydraulic conductance in southern California shrubs: a test of the hydraulic segmentation hypothesis. New Phytol 203:842–850

Pou A, Medrano H, Tomàs M, Martorell S, Ribas-Carbó M, Flexas J (2012) Anisohydric behaviour in grapevines results in better performance under moderate water stress and recovery than isohydric behaviour. Plant Soil 359:335–349

Reich PB (2014) The worldwide 'fast–slow' plant economics spectrum: a traits manifesto. J Ecol 102:275–301

Roman DT, Novick KA, Brzostek ER, Dragoni D, Rahman F, Phillips RP (2015) The role of isohydric and anisohydric species in determining ecosystem-scale response to severe drought. Oecologia 179:641–654

Sasani N, Pâques LE, Boulanger G, Singh AP, Gierlinger N, Rosner S, Brendel O (2021) Physiological and anatomical responses to drought stress differ between two larch species and their hybrid. Trees 35:1467–1484

Skelton RP, Dawson TE, Thompson SE, Shen Y, Weitz AP, Ackerly DD (2018) Low vulnerability to xylem embolism in leaves and stems of North American Oaks. Plant Physiol 177:1066–1077

Skelton RP, West AG, Dawson TE (2015) Predicting plant vulnerability to drought in biodiverse regions using functional traits. Proc Natl Acad Sci USA 112:5744–5749

Sperry J, Hacke U, Oren R, Comstock J (2002) Water deficits and hydraulic limits to leaf water supply. Plant Cell Environ 25:251–263

Sperry JS (2000) Hydraulic constraints on plant gas exchange. Agr Forest Meteorol 104:13–23

Streit K, Siegwolf RTW, Hagedorn F, Schaub M, Buchmann N (2014) Lack of photosynthetic or stomatal regulation after 9 years of elevated CO_2 and 4 years of soil warming in two conifer species at the alpine treeline. Plant Cell Environ 37:315–326

Tardieu F, Simonneau T (1998) Variability among species of stomatal control under fluctuating soil water status and evaporative demand: modelling isohydric and anisohydric behaviours. J Exp Bot 49:419–432

Tsuda M, Tyree MT (1997) Whole-plant hydraulic resistance and vulnerability segmentation in *Acer saccharinum*. Tree Physiol 17:351–357

Tyree MT, Ewers FW (1991) The hydraulic architecture of trees and other woody plants. New Phytol 119:345–360

Tyree MT, Hammel HT (1972) The measurement of the turgor pressure and the water relations of plants by the pressure-bomb technique. J Exp Bot 23:267–282

Urli M, Porte A, Cochard H, Guengant Y, Burlett R, Delzon S (2013) Xylem embolism threshold for catastrophic hydraulic failure in angiosperm trees. Tree Physiol 33:672–683

Wang AY, Wang M, Yang D, Song J, Zhang WW, Han SJ, Hao GY (2016) Responses of hydraulics at the whole-plant level to simulated nitrogen deposition of different levels in *Fraxinus mandshurica*. Tree Physiol 36:1045–1055

Wang CK, Han Y, Chen JQ, Wang XC, Zhang QZ, Bond-Lamberty B (2013) Seasonality of soil CO_2 efflux in a temperate forest: biophysical effects of snowpack and spring freeze–thaw cycles. Agr for Meteorol 177:83–92

Yi K, Dragoni D, Phillips RP, Roman DT, Novick KA (2017) Dynamics of stem water uptake among isohydric and anisohydric species experiencing a severe drought. Tree Physiol 37:1379–1392

Yoseph NA, Silvertown J, Gowing DJ, McConway KJ, Linder HP, Midgley G (2011) A fundamental, eco-hydrological basis for niche segregation in plant communities. New Phytol 189:253–258